

Article

Gas Sensor with Different Morphology of PANI Layer

Jiri Kroutil ^{1,*}, Alexandr Laposa ¹, Vojtech Povolny ¹, Ladislav Klimsa ²  and Miroslav Husak ¹

¹ Department of Microelectronics, Czech Technical University in Prague, Technicka 2, 166 27 Prague, Czech Republic

² Department of Material Analysis, FZU—Institute of Physics of the Czech Academy of Sciences, Na Slovance 1999/2, 182 00 Prague, Czech Republic

* Correspondence: kroutj1@fel.cvut.cz

Abstract: This work presents the design of a polymer-film-based sensor for gas detection. Different types of polyaniline are used as active layers. The advantages of resistive sensors with PANI layers are easy preparation and low production cost. At room temperature, polymer films have a high sensitivity to gas concentrations. The developed sensor works on the idea of electrical resistance shifting with gas concentration. Three different polymerization solutions are employed to synthesize the polyaniline (PANI) active layers (aqueous solution, sulfuric acid solution, and acetic acid solution). Active layers are evaluated in a controlled environment for their ability to detect ammonia, carbon monoxide, nitrogen monoxide, acetone, toluene, and relative humidity in synthetic air. PANI layers polymerized in acetic acid solutions exhibit good sensitivity toward ammonia.

Keywords: polyaniline; gas sensor; polymer film

1. Introduction

The monitoring of gaseous substances, especially toxic substances, is very important in many areas such as automotive, aviation, agriculture, security, health care, defense and security, industry, and environmental monitoring [1,2]. Ammonia, nitrogen oxides, organic volatiles, etc., are among those gasses. Medical applications of gas sensors include respiratory monitoring by analyzing carbon dioxide in exhaled air [3,4]. Active layers with organic materials achieve good sensitivity. Sensor requirements aim to make them smaller and more efficient. Research has focused on increasing resistance to gasses and higher temperatures. Polymer active layers are used in sensor arrays [5,6].

The active layers using conducting polymers are attractive for room temperature operations and easy synthesis. Sensing layers can be synthesized by various methods such as the co-precipitation method, the hydrothermal method, the sol-gel method, and microwave-assisted techniques [7]. Chemical sensors based on conducting polymers such as polyaniline (PANI), polypyrrole (PPy), and polythiophene (PTh) are suitable for their low cost, flexibility, light weight, and simple production [8]. PANI exhibits good stability in a wide range of conductivity and can be easily doped [9]. These features make polyaniline promising for industrial applications and for sensors with high selectivity, fast response times, recovery times, and the option to tailor its particular characteristics [10].

Polyaniline can form various oxidation states (fully oxidized pernigraniline, protoemeraldine, emeraldine, nigraniline, and fully reduced leucoemeraldine). The fully oxidized and reduced polyaniline is not conductive. A conducting emeraldine salt can be obtained, if the oxidation states are slightly doped (especially the emeraldine form) [11].

Low-cost printed sensors for clinical diagnostics and environmental monitoring can take advantage of the polymer active layers, such as low curing temperature (60 °C to 120 °C), thin and smooth films, low-cost production, light weight, and large-area applications [12,13].



Citation: Kroutil, J.; Laposa, A.; Povolny, V.; Klimsa, L.; Husak, M. Gas Sensor with Different Morphology of PANI Layer. *Sensors* **2023**, *23*, 1106. <https://doi.org/10.3390/s23031106>

Academic Editor: Victor Sysoev

Received: 31 December 2022

Revised: 11 January 2023

Accepted: 14 January 2023

Published: 18 January 2023



Copyright: © 2023 by the authors. Licensee MDPI, Basel, Switzerland. This article is an open access article distributed under the terms and conditions of the Creative Commons Attribution (CC BY) license (<https://creativecommons.org/licenses/by/4.0/>).

Detection of volatile organic compounds (VOCs) using PANI produced via in situ chemical polymerization was reported in [14]. This sensor is operated at room temperature. For the detection of ammonia gas, Safe et al. [15] fabricated a nanotube form of polyaniline with a response of 6% toward 20 ppm of ammonia.

Kumar et al. [16] prepared a PANI-based flexible sensor that detects ammonia in the range of 5–1000 ppm and operates at room temperature. In [17], the optimization of printed polyaniline for gas sensing applications was described. Hydrochloric acid-doped polyaniline was electrochemically synthesized and used as a gas sensor for ammonia in [18]. An ammonia gas sensor based on flexible PANI films was used for the rapid detection of spoilage in protein-rich foods [19]. In addition, polyaniline was doped with metals and metal oxides to increase sensing performance [20–22].

In this paper, we presented the design of a gas sensor with polyaniline layers prepared in different polymerization solutions: (i) aqueous solution, (ii) sulfuric acid solution, and (iii) acetic acid solution. Room temperature gas-sensing properties of the fabricated gas sensors to different gas environments (i.e., carbon oxide, carbon dioxide, ammonia, nitrogen dioxide, acetone, toluene, and relative humidity) were studied.

2. Materials and Methods

2.1. Materials

Isopropyl alcohol 99.8% ($(\text{CH}_3)_2\text{CHOH}$), acetone 99.5% (CH_3COCH_3), sulfuric acid 96% (H_2SO_4), acetic acid 99% ($\text{CH}_3\text{CO}_2\text{H}$), and hydrochloric acid 36% (HCl) were purchased from Penta Ltd. (Prague, Czech Republic). Ammonium persulfate 98% ($(\text{NH}_4)_2\text{S}_2\text{O}_8$) and aniline hydrochloride 98% ($\text{C}_6\text{H}_5\text{NH}_2 \text{HCl}$) were purchased from Lach-Ner Ltd. (Neratovice, Czech Republic).

2.2. Sensor Platform

The sensor platform KBI2 Tesla Blatná a. s. was used for the study of polyaniline layers (Figure 1). The sensor platform was fabricated by sputtering a thin layer of platinum on a $6.2 \text{ mm} \times 5.25 \text{ mm}$ ceramic substrate (Al_2O_3), followed by laser trimming to form the structures of the interdigital electrodes, temperature sensor (Pt1000), and heating element. The temperature sensor and the heating element were passivated by an insulating glass layer. Sensitive layers can be deposited on interdigital electrodes by various techniques, such as printing, dipping, screen printing, or immersion. In our study, we used the technique of dipping in a polymerization solution. The temperature element allows a constant temperature to be maintained or performs thermal cycling up to $450 \text{ }^\circ\text{C}$. The power consumption as a function of temperature can be seen in Figure 2. At $450 \text{ }^\circ\text{C}$, a sensor's power consumption is 3 W.

Figure 1b shows the structure of the sensor platform. The width and spacing of platinum ID (interdigital) electrodes are $15 \text{ }\mu\text{m}$. There are 80 individual electrode fingers (40 pairs), and the length of each is 2 mm.

2.3. Material Synthesis and Sensor Fabrication

The sensor platforms were cleaned with acetone and isopropyl alcohol for 15 min prior to the deposition of the sensing layer. At room temperature, 0.2 M aniline hydrochloride was oxidized with 0.25 M ammonium persulfate to produce polyaniline in the form of protonated emeraldine salt (Figure 3). This method was described in [9]. The polymerization was performed in different polymerization solutions: (i) aqueous solution, (ii) sulfuric acid solution, and (iii) acetic acid solution. Since polyaniline synthesis is an exothermic process, the temperature of the reaction mixture was monitored. The effect of temperature on PANI polymerization time is shown in Figure 4. The process of polymerization was finished at $37 \text{ }^\circ\text{C}$ within 15 min for the aqueous solution, at $36 \text{ }^\circ\text{C}$ within 10 min for the sulfuric acid solution, and at $35 \text{ }^\circ\text{C}$ within 25 min for the acetic acid solution. Before drying the sensors on a hotplate at $60 \text{ }^\circ\text{C}$ for 2 h and then by silica gel in a desiccator for 24 h, they were purified using 0.2 M hydrochloric acid and acetone.

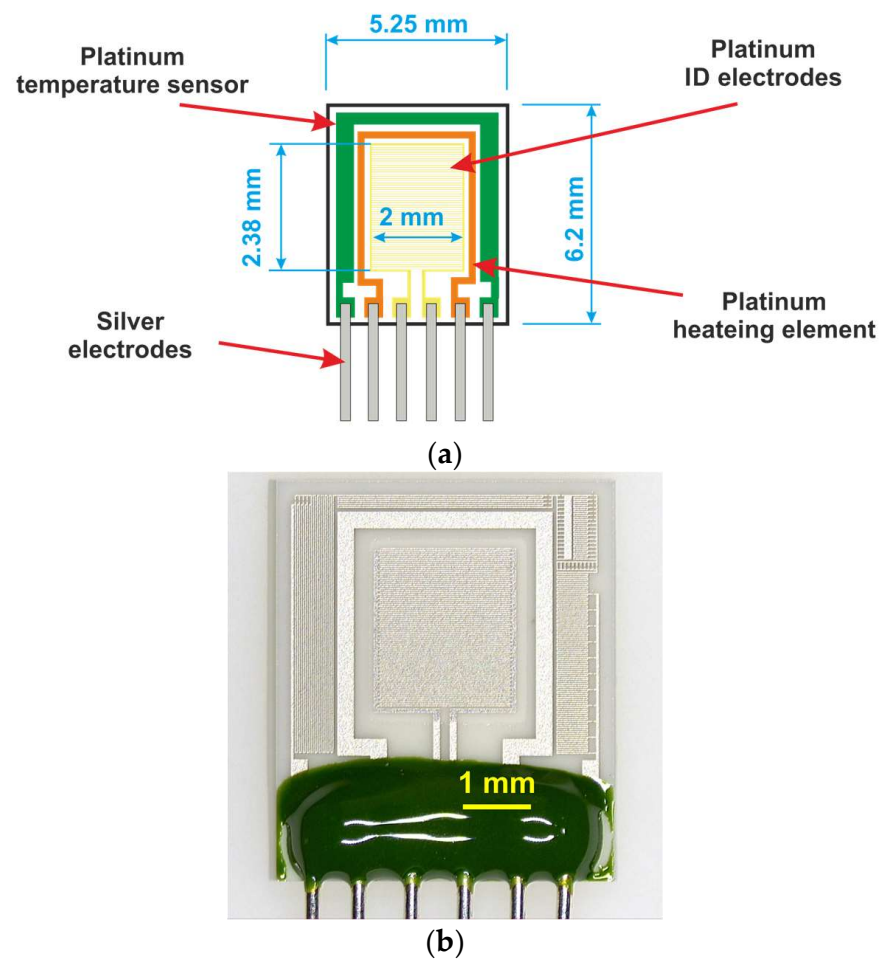


Figure 1. Sensor platform KBI2 Tesla Blatná: (a) the schematic diagram with dimensions, (b) sensor platform without a sensitive layer.

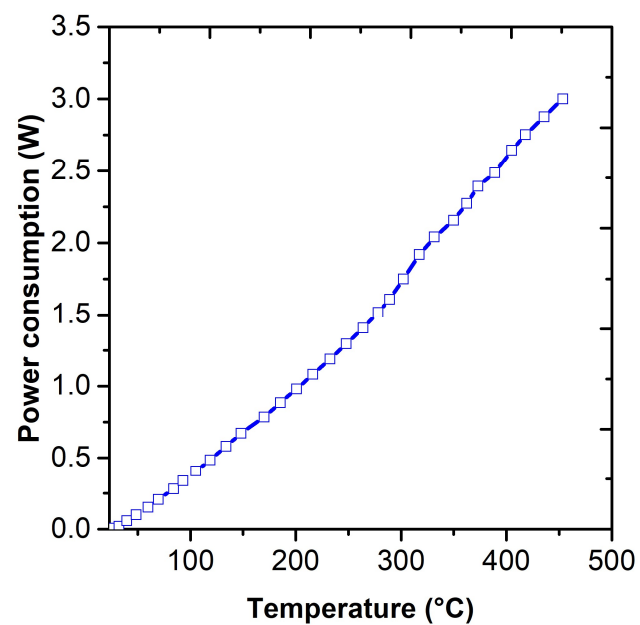


Figure 2. Dependence of the power consumption on the temperature.

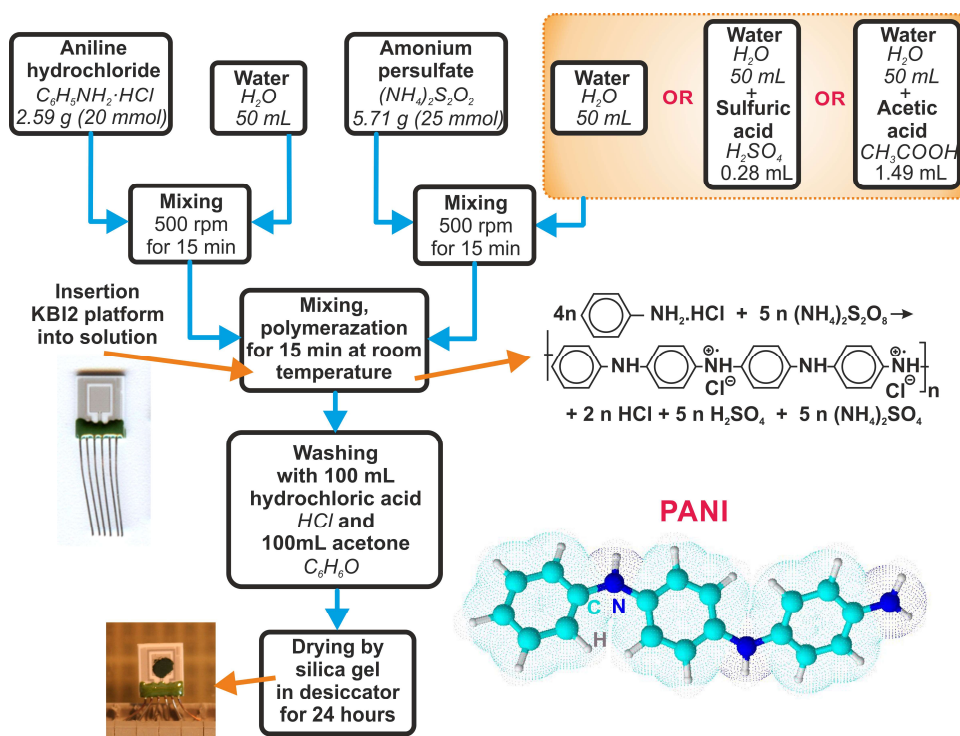


Figure 3. Preparation of various forms of polyaniline.

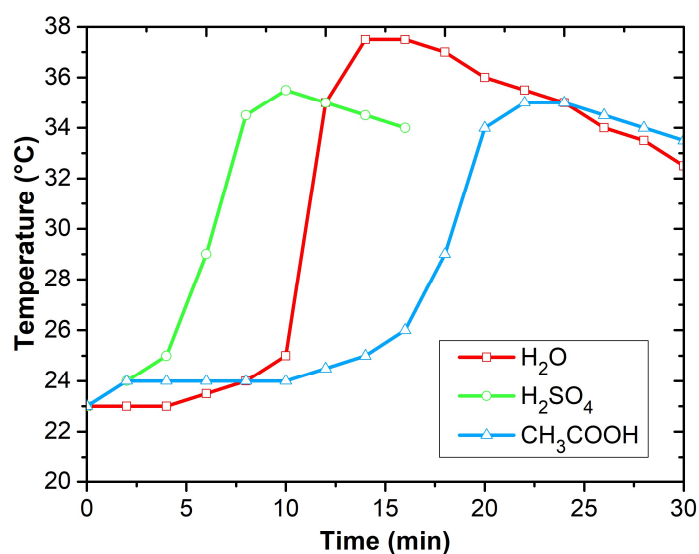


Figure 4. The temperature of the reaction mixture as a function of time.

2.4. Preparation of the Gas Testing System

A measuring apparatus was designed for testing the gas sensors (Figure 5). The apparatus allows for the precise adjustment of gas concentrations using Bronkhorst mass flow controllers MFC1 to MFC3 (F-201DV-AAD-22-K in the range 10 mL–500 mL, F-201EV-AAD-22-K in the range 40 mL–2000 mL). Synthetic air (SA: 21% O₂ and the rest N₂) is used as a carrier gas, which also serves as a purging gas. The exact concentration of the test gas can be obtained by mixing it with the carrier gas or by diluting the saturated vapor of the desired solvent from the bubbler with dry air. This second method is mainly used to generate different concentrations of humidity and volatile compounds (ethanol, methanol, acetone, toluene, cyclohexane, etc.). The resulting mixture is then injected into the test chamber with the tested sensor. The volume of the test chamber is 50 mL. A Keithley 2400 sourcemeter

was used to measure the resistance. A relay multiplexer is used to switch individual sensors, which is controlled by a National Instruments USB-6351 DAQ (Data Acquisition) device (16 analog inputs, 24 digital inputs/outputs, 2 analog outputs, maximum sampling rate 125 MS/s). The resistance values of the sensors are measured every 250 ms. The connection of the sensors between the multiplexer and the sourcemeter is performed using a coaxial cable to reduce interference from external electromagnetic fields. The VICI EUTA-4VL4MWE2 four-port two-way valve is used to switch the flow of gasses (test gas–purge gas) to ensure a rapid increase to the target concentration of the test gas, and to avoid the influence of overflows during switching. The apparatus and measurement process are controlled by the LabView application.

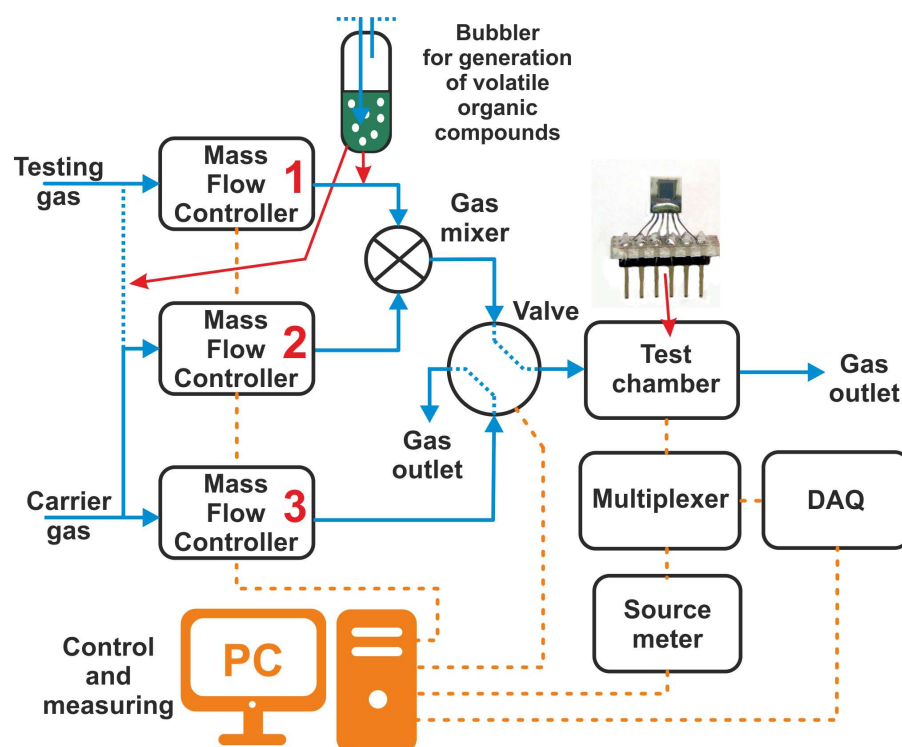


Figure 5. Schematic diagram of the gas sensing characterizations apparatus.

The change in sensor resistance ($\Delta R/R_0$) as a function of exposure time was investigated. The response of the sensor is given by the change in relative resistance,

$$\Delta R/R_0 = (R_g - R_0)/R_0, \quad (1)$$

where R_g represents the resistances upon exposure to a specific gas and R_0 is the reference resistances in synthetic gas. The fabricated sensors were used for the detection of ammonia (NH_3), carbon dioxide (CO_2), nitrogen dioxide (NO_2), acetone (CH_3COCH_3), toluene ($\text{C}_6\text{H}_5\text{CH}_3$), and humid air (RH) under various concentrations at room temperature.

3. Results and Discussion

3.1. Scanning Electron Microscopy (SEM) and Raman Spectroscopy

Scanning electron microscopy (SEM, TESCAN FERA3 GM) was used to analyze the surface morphology of the deposited active layers (Figure 6a–c). All active PANI layers have nanostructure morphologies, especially when polymerized in sulfuric acid solution and acetic acid solution. Polyaniline synthesized in an aqueous solution forms a granular form, while that synthesized in an acidic environment forms nanotubes. Polyaniline prepared in acetic acid exhibits the highest proportion of nanotubes.

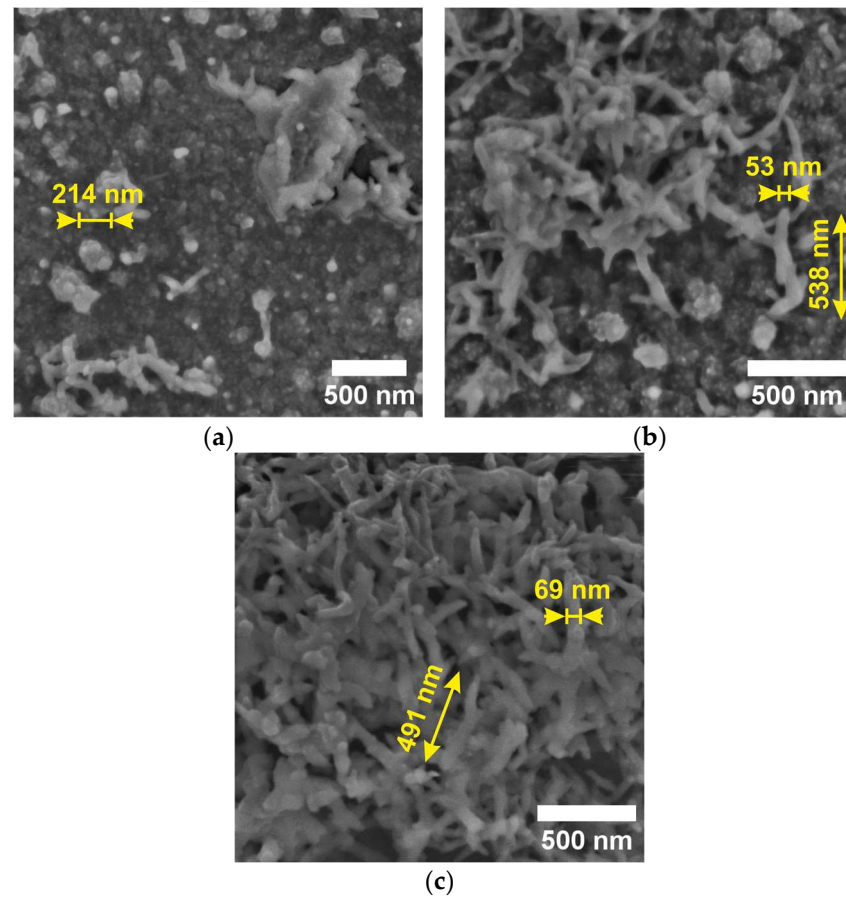


Figure 6. SEM micrographs of the deposited active layers surface morphology polymerized in: (a) aqueous solution, (b) sulfuric acid, and (c) acetic acid.

The PANI layers were also examined by Raman spectroscopy to confirm the deposited sensitive layers and their purity. Raman spectroscopy was performed at room temperature using a Renishaw inVia Qontor Raman spectrometer at a wavelength of 633 nm. The obtained spectra are shown in Figure 7. The spectrum of pristine PANI with main bands is described in Table 1 [23,24].

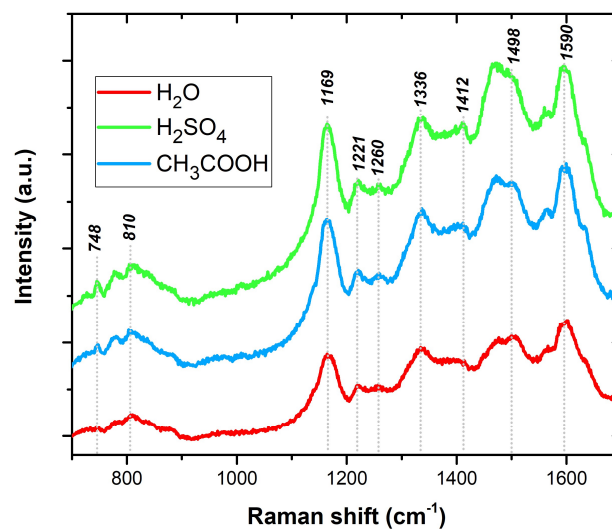


Figure 7. The Raman spectra of the PANI layers.

Table 1. Values of the average temperature coefficients of the sensitive polyaniline layers in a temperature range from 23 °C to 80 °C.

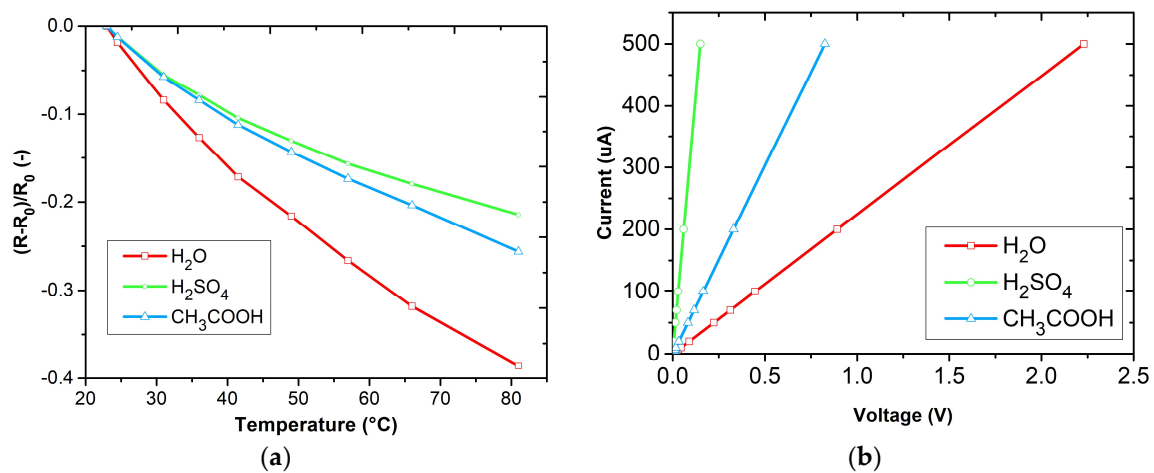
Raman Shift (cm ⁻¹)	Description of Band
748	Q ring bending, C–C ring deformation
810	out-of-plane C–H vibrations in the aromatic rings
1169	C–H bending of the quinoid rings
1221	C–N in benzene diamine units
1260	C–N in benzene diamine units
1336	C–N ⁺ , a characteristic band of the polaron radical cation
1412	phenazine structures
1498	C=N of the quinoid nonprotonated diimine units
1590	C=C stretching vibration of the quinonoid ring

3.2. Temperature Analysis and Current-Voltage Characteristics of Polyaniline Layers

The temperature dependencies of the prepared layers are shown in Figure 8a. The average values of the temperature coefficients of resistance (TCR) can be determined according to:

$$\Delta R/R_0 = \alpha \cdot \Delta T, \quad (2)$$

where α is the temperature coefficient, ΔR is the difference in electrical resistance over a given temperature range, R_0 is the initial temperature, and ΔT is the temperature range. Table 2 shows the average values of the temperature coefficients of the different sensitive PANI layers in a temperature range from 23 °C to 80 °C.

**Figure 8.** Temperature dependencies of sensitive layers (a) and current-voltage characteristics of sensitive layers (b).**Table 2.** Values of the average temperature coefficients of the sensitive polyaniline layers in a temperature range from 23 °C to 80 °C.

Sensitive Layer	α (K ⁻¹)
PANI polymerized in H ₂ O	−0.0066
PANI polymerized in H ₂ SO ₄	−0.0038
PANI polymerized in CH ₃ COOH	−0.0044

The temperature dependencies of the polyaniline layers exhibit a negative temperature coefficient. The polyanilines formed in acidic environments have a lower temperature dependence than the PANI formed in aqueous environments. The temperature dependencies

show an exponential behavior, which is consistent with the temperature dependence of polyaniline described by the equation [25].

$$\sigma = \sigma_0 \cdot \exp(-(T_0/T)^{(1/d+1)}), \quad (3)$$

where σ is the specific conductance, d is the dimension of the sample, σ_0 and T_0 are the parameters. If the sample is three-dimensional, we obtain the so-called Mott relation of temperature dependence, where the exponent is equal to:

$$1/d + 1 = 4 \quad (4)$$

The current-voltage characteristics shown in Figure 8b exhibit linear dependencies. The electrical resistance of the polyaniline layers at 25 °C and 50% relative humidity are shown in Table 3. It indicates that polyaniline formed in acidic media has lower electrical resistance than polyaniline formed in an aqueous solution.

Table 3. Electrical resistance values of sensitive polyaniline layers at 25 °C and 50 % relative humidity.

Sensitive Layer	R (Ω)
PANI polymerized in H ₂ O	4470
PANI polymerized in H ₂ SO ₄	306
PANI polymerized in CH ₃ COOH	1660

3.3. Gas Sensing Analysis

The DC analysis was performed due to the expected use of the sensors in applications working with a DC power supply and the possibility of simple evaluation. The electrical resistance was measured as a function of the time changes in the gas concentrations. Figure 9a–d shows the responses of PANI layers toward ammonia (12.5 ppm NH₃), carbon monoxide (12.5 ppm CO), carbon dioxide (250 ppm CO₂), and nitrogen dioxide (12.5 ppm NO₂). The sensitive layers were also tested with volatile organic compounds (VOCs), 0.6% of acetone, 0.05% of toluene (Figure 10a,b), and toward humidity (Figure 11). Three cycles with the specified concentrations (5 min of exposure to the test gas, 5 min of synthetic air (SA) purging, flow rate 100 mL·s⁻¹) were performed during the testing. The measuring current was set to 10 μA to reduce the possibility of heating the layers.

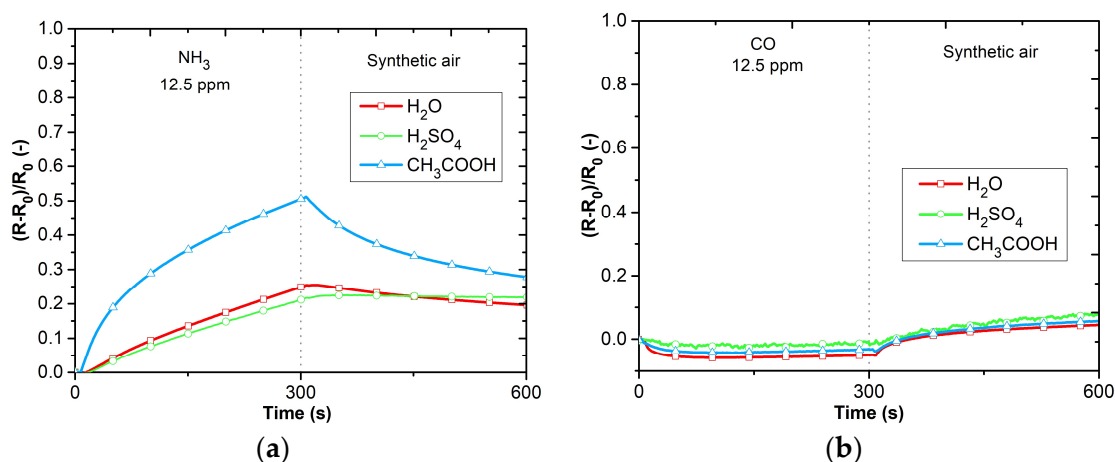


Figure 9. Cont.

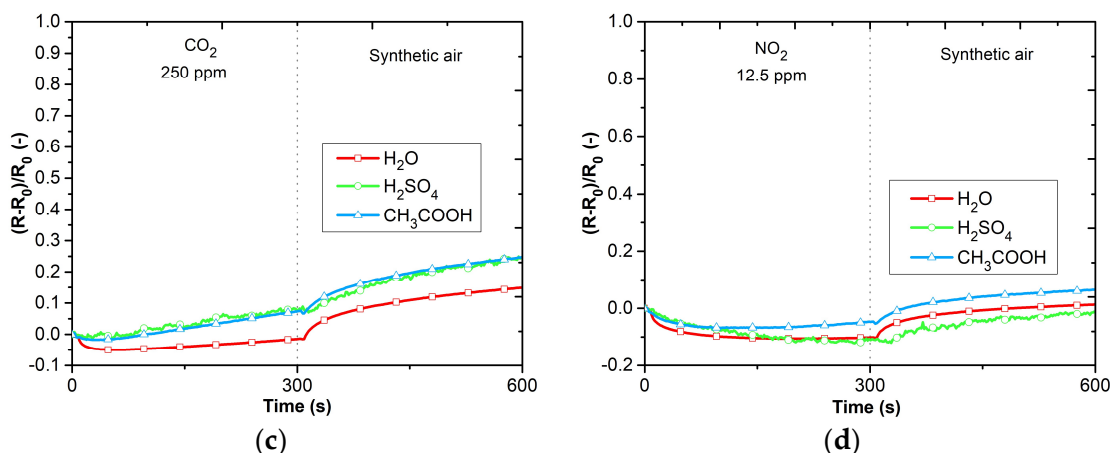


Figure 9. Responses of active layers: (a) reaction to NH₃, (b) reaction to CO, (c) reaction to CO₂, (d) reaction to NO₂.

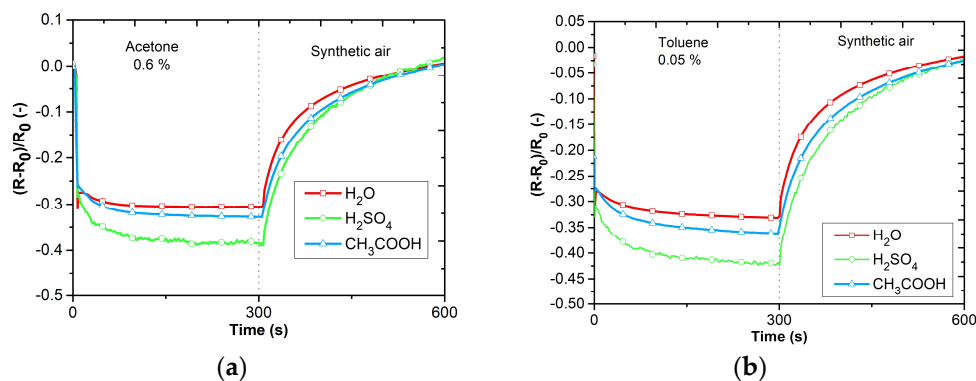


Figure 10. Responses of active layers toward VOCs: (a) reaction to acetone, (b) reaction to toluene.

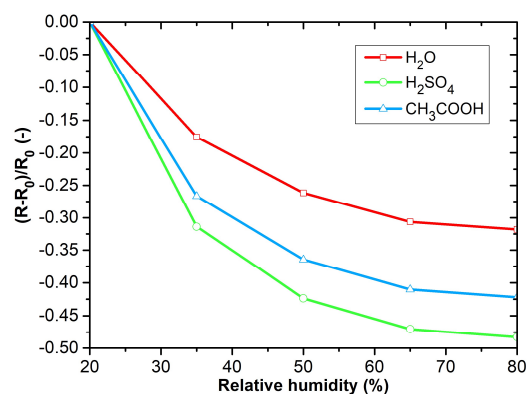


Figure 11. RH dependences of active layers.

The active layers exhibit the highest sensitivity to ammonia (Figure 9a). Polyaniline polymerized in acetic acid exhibits the greatest sensitivity. The reactions to carbon monoxide, carbon dioxide, and nitrogen dioxide show low sensitivity (Figure 9b–d). Significant sensitivity can be observed to acetone, toluene, and humidity (Figures 10a,b and 11). PANI layers exhibit a relatively fast response time to VOCs. Electrical resistance decreases with increasing relative humidity.

Ammonia is a gas generally detected by PANI layers because the nitrogen atoms of both compounds play a similar role in forming coordination bonds with protons. The deprotonation/protonation mechanism is used to explain the sensitivity and reversibility of the mineral acid-doped PANI layer to ammonia (Figure 12). The free nitrogen doublet of

the ammonia molecule can form a coordination bond with the free atomic orbital of the donating proton. This reaction leads to the deprotonation of the polyaniline nitrogen atoms, involving the removal of charge carriers (polarons) and an increase in electrical resistance. Moreover, it may participate in the gas swelling reaction of the polymer [26].

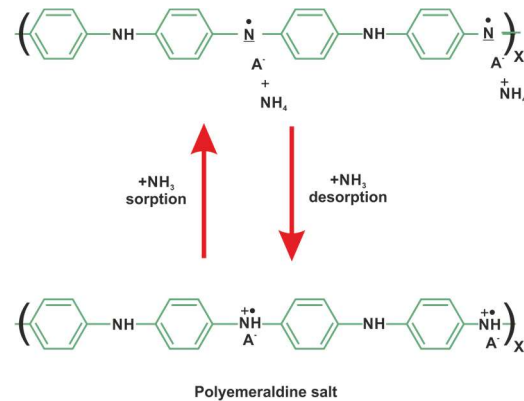


Figure 12. The reaction of PANI endowed with HA mineral acids ($A=Cl, HSO_4, ClO_4$, etc.) to ammonia [26].

Due to high sensitivity to ammonia, the sensing layers were further tested at both room temperature (Figure 13a) and at a higher temperature of 80 °C (Figure 13b) for various concentrations. When the layers are exposed to elevated temperatures up to 80 °C during testing with ammonia, a relatively good recovery of the sensor resistance to the initial value is observed. This can be explained by the better desorption of gas from the sensitive layer by supplying thermal energy. Figure 14 shows the response of the sensor layers to repeating the same ammonia concentration (12.5 ppm). The repeatability of the sensitive layer responses is observed from these waveforms.

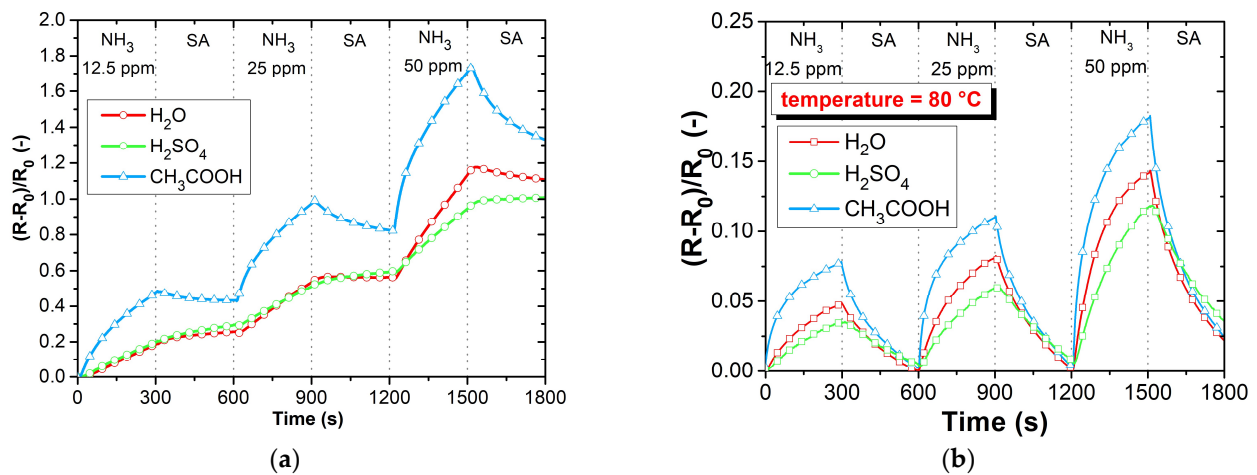


Figure 13. Gas characterization of active layers toward ammonia: (a) various concentrations at room temperature, (b) various concentrations at 80 °C.

Figure 15 summarizes the responses of the PANI layers to the tested gases. High sensitivity is evident for ammonia, especially for PANI polymerized in acetic acid. Furthermore, it can be observed that ammonia is a reducing gas, while the other tested gases have an oxidizing character. Similar reduction behavior was observed for chloroform [27] and hydrogen sulfide [28]. Increased sensitivity to higher concentrations of acetone and toluene can also be observed.

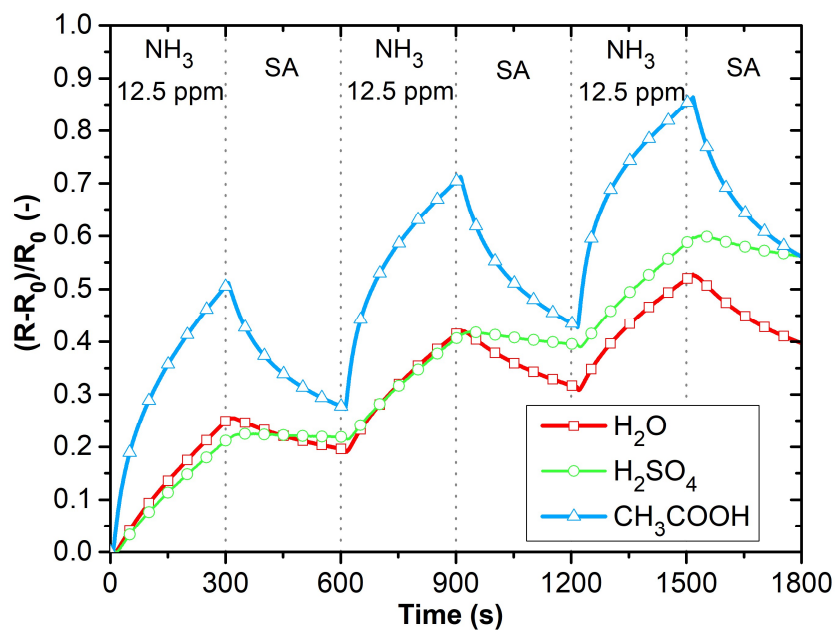


Figure 14. Gas characterization of active layers toward 12.5 ppm of ammonia.

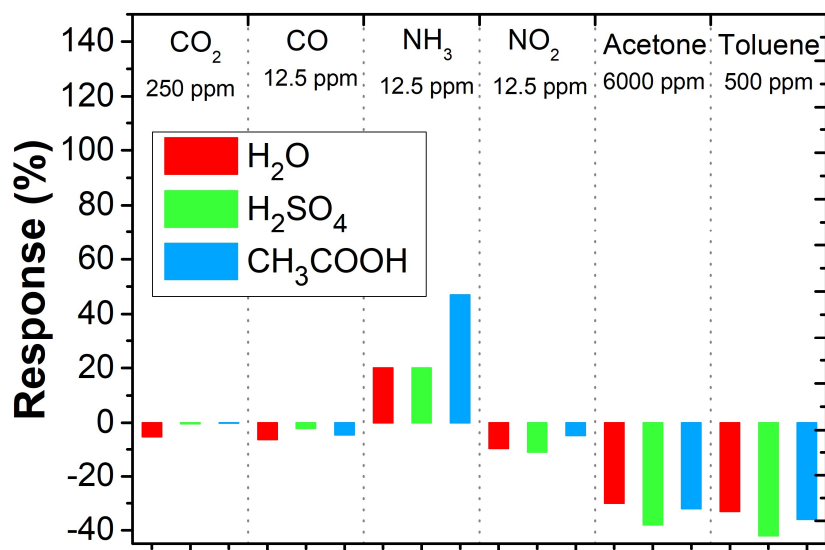


Figure 15. Overview of PANI layer response toward tested gasses and vapors.

Our results were compared with similar works, as shown in Table 4. In [29], PANI doped with acrylic acid was synthesized and its production was described. The layer was exposed to various concentrations of ammonia from 1 ppm to 600 ppm. The sensor response was $\Delta R/R_0 = 0.99$ for a concentration of 58 ppm. Measurements were performed at room temperature. In [30], a sensor on a flexible substrate with a PANI sensitive layer was prepared. The authors used inkjet technology (modified Epson C46/C48 printer) for the deposition of PANI on the substrate. A response to an ammonia concentration of 50 ppm at 70 °C $\Delta R/R_0 = 0.99$ was achieved. Responses $\Delta R/R_0 = 0.3$ [31] and $\Delta R/R_0 = 0.8$ [32] were achieved using PANI doped with dodecylbenzenesulfonic acid. In [33], nanofibers doped with hydrochloric acid were created and the sensor response achieved $\Delta R/R_0 = 2.9$ at 50 °C.

Table 4. Comparison of implemented sensors with other works.

PANI Preparation Technology	Deposition Method of PANI	Substrate	Electrode Material	NH ₃ Concentration (ppm)	Operating Temperature (°C)	Relative Humidity (%)	Response $\Delta R/R_0$ (-)	Time Responses/Recovery (s)	Ref.
PANI acrylic acid-doped	-	-	-	58	25	-	0.99	60/240	[29]
Ink-jet printing	Ink-jet	PET	Ag	50	70	-	0.15	100/200	[30]
PANI doped with dodecylbenzenesulfonic acid	Spin coating	Polyester (Tartan 950)	MWCNT ink	20	28	45	0.15	300/900	[31]
PANI doped with dodecylbenzenesulfonic acid	data	Al ₂ O ₃	Au	50	25	Dry air	0.8	90/180	[32]
PANI nanofibers doped with HCl	Spin coating	Al ₂ O ₃	Au	200	50	Dry N ₂	2.9	600/300	[33]
PANI prepared by polymerization in solution on a substrate	Coating during polymerization	Al ₂ O ₃	Pt	50	25	Dry synthetic air	0.85	300/-	Our work

4. Conclusions

In this paper, we demonstrated the fabrication and characterization of gas sensors with polyaniline active layers. These layers were polymerized in different polymerization solutions: aqueous, sulfuric acid, and acetic acid. Commercial Tesla Blatná platforms were used for sensors with polyaniline layers that were inserted into the polymerization solution during polymerization. These were coated with sensitive PANI layers. The sensor could be prepared with such sensitive layers in a single step, which is a significant benefit.

The surface morphology of these layers was examined using a scanning electron microscope. Polyaniline synthesized in an aqueous solution formed a granular form and in an acidic environment formed nanotubes. PANI layers polymerized in an acidic solution exhibited lower temperature sensitivity.

The polyaniline sensor was tested for the detection of CO, CO₂, NH₃, NO₂, acetone, and toluene. The highest response was obtained for polyaniline polymerized in acetic acid toward ammonia ($\Delta R/R_0 = 0.95$ for 50 ppm of NH₃). Better reversibility could be obtained at higher operating temperatures.

Author Contributions: Conceptualization, J.K. and M.H.; methodology, J.K. and A.L.; characterization J.K., A.L., V.P. and L.K.; investigation, J.K., A.L., V.P. and L.K.; writing—original draft preparation, J.K.; writing—review and editing, A.L., V.P. and L.K. All authors have read and agreed to the published version of the manuscript.

Funding: This work was supported by the Czech Science Foundation project No. GA22-04533S “Printed heterogeneous gas sensor arrays with enhanced sensitivity and selectivity” and by the CzechNanoLab Research Infrastructure LM2018110.

Institutional Review Board Statement: Not applicable.

Informed Consent Statement: Not applicable.

Data Availability Statement: Not applicable.

Conflicts of Interest: The authors declare no conflict of interest.

Abbreviations

The following abbreviations are used in this manuscript:

DAQ	Data Acquisition
DC	Direct Current
ID	Interdigital
PANI	Polyaniline
PPy	Polypyrrole
PTh	Polythiophene
SA	Synthetic air
SEM	Scanning electron microscopy
VOC	Volatile Organic Compounds

References

1. Hosseini, S.H.; Khalkhali, R.A.; Noor, P. Study of polyaniline conducting/electroactive polymer as sensor for some agricultural phosphorus pesticides. *Mon. Fur Chem.* **2010**, *141*, 1049–1053. [[CrossRef](#)]
2. Akbar, S.; Dutta, P.; Lee, C. High-temperature ceramic gas sensors: A review. *Int. J. Appl. Ceram. Technol.* **2006**, *3*, 302–311. [[CrossRef](#)]
3. Tatara, T.; Tsuzaki, K. An apnea monitor using a rapid-response hygrometer. *J. Clin. Monit.* **1997**, *13*, 5–9. [[CrossRef](#)] [[PubMed](#)]
4. Ma, Y.; Ma, S.; Wang, T.; Fang, W. Air-flow sensor and humidity sensor application to neonatal infant respiration monitoring. *Sens. Actuators A Phys.* **1995**, *49*, 47–50. [[CrossRef](#)]
5. Sun, Y.; Ong, K.Y. *Detection Technologies for Chemical Warfare Agents and Toxic Vapors*; CRC Press: Boca Raton, FL, USA, 2005; ISBN 9780203485705 020348570X.
6. Kroutil, J.; Laposka, A.; Voves, J.; Davydova, M.; Nahlik, J.; Kulha, P.; Husak, M. Performance Evaluation of Low-Cost Flexible Gas Sensor Array with Nanocomposite Polyaniline Films. *IEEE Sens. J.* **2018**, *18*, 3759–3766. [[CrossRef](#)]
7. Gupta, A.; Verma, G. *Nanostructured Gas Sensors*; Jenny Stanford Publishing: New York, NY, USA, 2022; ISBN 9781003331230.
8. Nagaraju, S.C.; Roy, A.S.; Kumar, J.B.P.; Anilkumar, K.R.; Ramagopal, G. Humidity Sensing Properties of Surface Modified Polyaniline Metal Oxide Composites. *J. Eng.* **2014**, *2014*, 925020. [[CrossRef](#)]
9. Stejskal, J.; Gilbert, R.G. Polyaniline. Preparation of a conducting polymer (IUPAC Technical Report). *Pure Appl. Chem.* **2002**, *74*, 857867. [[CrossRef](#)]
10. Fratoddi, I.; Venditti, I.; Cametti, C.; Russo, M.V. Chemiresistive polyaniline-based gas sensors: A mini review. *Sens. Actuators B Chem.* **2015**, *220*, 534–548. [[CrossRef](#)]
11. Feast, W.J.; Tsibouklis, J.; Pouwer, K.L.; Groenendaal, L.; Meijer, E.W. Synthesis, processing and material properties of conjugated polymers. *Polymer* **1996**, *37*, 5017–5047. [[CrossRef](#)]
12. Crowley, K.; Smyth, M.; Killard, A.; Morrin, A. Printing polyaniline for sensor applications. *Chem. Pap.* **2013**, *67*, 771–780. [[CrossRef](#)]
13. Kang, H.; Park, H.; Park, Y.; Jung, M.; Kim, B.C.; Wallace, G.; Cho, G. Fully Roll-to-Roll Gravure Printable Wireless (13.56 MHz) Sensor-Signage Tags for Smart Packaging. *Sci. Rep.* **2015**, *4*, 5387. [[CrossRef](#)] [[PubMed](#)]
14. Kashyap, R.; Kumar, R.; Kumar, M.; Tyagi, S.; Kumar, D. Polyaniline nanofibers based gas sensor for detection of volatile organic compounds at room temperature. *Mater. Res. Express* **2019**, *6*, 1150d3. [[CrossRef](#)]
15. Safe, A.M.; Ahmadi Tabar, F.; Nikfarjam, A.; Sharif, F.; Hajghassem, H.; Mazinani, S. Hollow Polyaniline Nanofibers for Highly Sensitive Ammonia Detection Applications. *IEEE Sens. J.* **2019**, *19*, 9616–9623. [[CrossRef](#)]
16. Kumar, L.; Rawal, I.; Kaur, A.; Annapoorni, S. Flexible room temperature ammonia sensor based on polyaniline. *Sens. Actuators B Chem.* **2017**, *240*, 408–416. [[CrossRef](#)]
17. Reiner-Rozman, C.; Pichler, B.; Madi, V.; Weißenböck, P.; Hegedüs, T.; Aspermaier, P.; Binting, J. Optimization of Printed Polyaniline Composites for Gas Sensing Applications. *Sensors* **2022**, *22*, 5379. [[CrossRef](#)]
18. Korent, A.; Žagar Soderžnik, K.; Šturm, S.; Žužek Rožman, K.; Redon, N.; Wojkiewicz, J.-L.; Duc, C. Facile Fabrication of an Ammonia-Gas Sensor Using Electrochemically Synthesised Polyaniline on Commercial Screen-Printed Three-Electrode Systems. *Sensors* **2020**, *21*, 169. [[CrossRef](#)]
19. Matindoust, S.; Farzi, A.; Baghaei Nejad, M.; Shahrokh Abadi, M.H.; Zou, Z.; Zheng, L.-R. Ammonia gas sensor based on flexible polyaniline films for rapid detection of spoilage in protein-rich foods. *J. Mater. Sci. Mater. Electron.* **2017**, *28*, 7760–7768. [[CrossRef](#)]
20. Liu, J.; Cui, N.; Xu, Q.; Wang, Z.; Gu, L.; Dou, W. High-Performance PANI-Based Ammonia Gas Sensor Promoted by Surface Nanostructuralization. *ECS J. Solid State Sci. Technol.* **2021**, *10*, 027007. [[CrossRef](#)]
21. Wang, X.; Gong, L.; Zhang, D.; Fan, X.; Jin, Y.; Guo, L. Room temperature ammonia gas sensor based on polyaniline/copper ferrite binary nanocomposites. *Sens. Actuators B Chem.* **2020**, *322*, 128615. [[CrossRef](#)]
22. Zhang, W.; Cao, S.; Wu, Z.; Zhang, M.; Cao, Y.; Guo, J.; Zhong, F.; Duan, H.; Jia, D. High-Performance Gas Sensor of Polyaniline/Carbon Nanotube Composites Promoted by Interface Engineering. *Sensors* **2019**, *20*, 149. [[CrossRef](#)]

23. Salvatierra, R.V.; Moura, L.G.; Oliveira, M.M.; Pimenta, M.A.; Zabin, A.J.G. Resonant Raman spectroscopy and spectroelectrochemistry characterization of carbon nanotubes/polyaniline thin film obtained through interfacial polymerization. *J. Raman Spectrosc.* **2012**, *43*, 1094–1100. [[CrossRef](#)]
24. Trchová, M.; Morávková, Z.; Bláha, M.; Stejskal, J. Raman spectroscopy of polyaniline and oligoaniline thin films. *Electrochim. Acta* **2014**, *122*, 28–38. [[CrossRef](#)]
25. Inzelt, G. *Conducting Polymers: A New Era in Electrochemistry*; Springer: Berlin/Heidelberg, Germany, 2008. [[CrossRef](#)]
26. Nicolas-Debarnot, D.; Poncin-Epaillard, F. Polyaniline as a new sensitive layer for gas sensors. *Anal. Chim. Acta* **2003**, *475*, 1–15. [[CrossRef](#)]
27. Virji, S.; Huang, J.; Kaner, R.B.; Weiller, B.H. Polyaniline Nanofiber Gas Sensors: Examination of Response Mechanisms. *Nano Lett.* **2004**, *4*, 491–496. [[CrossRef](#)]
28. Akber, H.J.; Ibrahim, I.M.; Razeg, K.H. Hydrothermal Synthesis of Polyaniline Nano-fibers as H₂S Gas Sensor. *J. Phys. Conf. Ser.* **2020**, *1664*, 012017. [[CrossRef](#)]
29. Chabukswar, V.V.; Pethkar, S.; Athawale, A.A. Acrylic acid doped polyaniline as an ammonia sensor. *Sens. Actuators B Chem.* **2001**, *77*, 657–663. [[CrossRef](#)]
30. Crowley, K.; Morrin, A.; Hernandez, A.; O'Malley, E.; Whitten, P.G.; Wallace, G.G.; Smyth, M.R.; Killard, A.J. Fabrication of an ammonia gas sensor using inkjet-printed polyaniline nanoparticles. *Talanta* **2008**, *77*, 710–717. [[CrossRef](#)]
31. Rizzo, G.; Arena, A.; Donato, N.; Latino, M.; Saitta, G.; Bonavita, A.; Neri, G. Flexible, all-organic ammonia sensor based on dodecylbenzene sulfonic acid-doped polyaniline films. *Thin Solid Film.* **2010**, *518*, 7133–7137. [[CrossRef](#)]
32. Wu, S.; Zeng, F.; Li, F.; Zhu, Y. Ammonia sensitivity of polyaniline films via emulsion polymerization. *Eur. Polym. J.* **2000**, *36*, 679–683. [[CrossRef](#)]
33. Matsuguchi, M.; Asahi, T. Properties and stability of polyaniline nanofiber ammonia sensors fabricated by novel on-substrate method. *Sens. Actuators B Chem.* **2011**, *160*, 999–1004. [[CrossRef](#)]

Disclaimer/Publisher's Note: The statements, opinions and data contained in all publications are solely those of the individual author(s) and contributor(s) and not of MDPI and/or the editor(s). MDPI and/or the editor(s) disclaim responsibility for any injury to people or property resulting from any ideas, methods, instructions or products referred to in the content.